DMD Fast Forward. Published on February 12, 2007 as doi:10.1124/dmd.106.013805

OXIDATION OF VINYL CARBAMATE AND FORMATION OF 1,N^6-ETHENODEOXYADENOSINE IN MURINE LUNG

Poh-Gek Forkert, Martin Kaufmann, Gordon Black, Raymond Bowers, Heidi Chen, Kathy Collins, Ashish Sharma and Glenville Jones

Departments of Anatomy and Cell Biology (P.G.F., G.B., K.C., A.S.), Biochemistry (M.K., G.J.) and Chemistry (R.B.), Queen's University, Kingston, Ontario, Canada; Food Research Division (H.C.), Bureau of Chemical Safety, Health Canada, Ottawa, Ontario, Canada

DMD Fast Forward. Published on February 12, 2007 as DOI: 10.1124/dmd.106.013805
This article has not been copyedited and formatted. The final version may differ from this version.

Running Title: Formation of 1,N^6-Ethenodeoxyadenosine from Vinyl Carbamate

Address correspondence to: Dr. Poh-Gek Forkert

Department of Anatomy and Cell Biology

Queen's University, Kingston, Ontario

Canada K7L 3N6

Phone: (613) 533-2854

Fax: (613) 533-2566

Email: forkertp@post.queensu.ca

Text pages	29
Tables	0
Figures	7
References	39
Abstract	250
Introduction	766
Discussion	1491
Section assignment	Toxicology

ABBREVIATIONS: dAS, 2′-deoxyadenosine; DDAS, 2′-deoxy-2-deuteroethenoadenosine; $DASO_2$, diallyl sulfone; εdAS, 1,N^6-ethenodeoxyadenosine; EC, ethyl carbamate; HPLC, high performance liquid chromatography; LC-MS, high performance liquid chromatography-mass spectrometry; LC-MS/MS, high performance liquid chromatography-mass spectrometry/mass spectrometry; *m*CPBA, *m*-chloroperoxybenzoic acid; MRM, multiple reaction monitoring; VC, vinyl carbamate; VCO, vinyl carbamate epoxide.

DMD Fast Forward. Published on February 12, 2007 as DOI: 10.1124/dmd.106.013805
This article has not been copyedited and formatted. The final version may differ from this version.

ABSTRACT:

Vinyl carbamate (VC) is derived from ethyl carbamate, a carcinogen formed in fermentation of food and alcoholic products. We have undertaken studies to test the hypothesis that an epoxide generated from VC oxidation leads to formation of 1,N^6-ethenodeoxyadenosine (εdAS). We have developed approaches using LC-MS and LC-MS/MS for identification and quantitation of εdAS. Scanning and fragment ion analyses confirmed the identity of εdAS based on the molecular ion $[M+H]^+$ *m/z* 276 and the specific fragment ion *m/z* 160. Chemical oxidation of VC in reactions containing 2′-deoxyadenosine produced εdAS with ^{1}H-NMR, chromatographic and mass spectral characteristics identical to the authentic εdAS, suggesting DNA alkylation by the VC epoxide. Subsequent studies evaluated formation of εdAS in incubations of murine lung microsomes or recombinant CYP2E1 with VC. The formation of εdAS in incubations of lung microsomes or recombinant CYP2E1 with VC was dependent on protein concentrations, CYP2E1 enzyme levels and incubation time. The rates of εdAS formation were highly correlated with VC concentrations. Peak rates were produced by lung microsomes and recombinant CYP2E1 at 3.0 and 2.5 mM of VC, respectively. In inhibitory studies, incubations of VC were performed using lung microsomes from mice treated with the CYP2E1 inhibitor diallyl sulfone (100 mg/kg, p.o.). Results from these studies showed significantly decreased εdAS formation in microsomes incubated with VC, with an inhibition of 70% at 3.0 mM. These findings suggested that CYP2E1 is a major enzyme mediating VC oxidation, leading to the formation of a metabolite that alkylates DNA to form the εdAS adduct.

Vinyl carbamate (VC) is a metabolite and structural analog of ethyl carbamate (EC), a byproduct of fermentation found in alcoholic beverages and a variety of food products including yoghurt, bread, soya sauce, cheese and apple cider vinegar (Ough, 1976; Battaglia et al., 1990; Zimmerli and Schlatter, 1991). The highest concentrations of EC (100-20,000 ng/g) were detected in alcoholic beverages including stone-fruit brandies (plums, apricots or cherries), sherry and bourbon. It is also found as a natural constituent in tobacco at concentrations ranging from 310-375 ng/g (Schmeltz et al., 1978). It has been estimated that the mean daily intake of EC from various food items in adults is about 10-20 ng/kg of body weight (Zimmerli and Schlatter, 1991).

The carcinogenicity of EC and the formation of lung adenomas in animals were first reported in 1943 (Nettleship et al., 1943). Subsequent studies in mice demonstrated that EC induces tumors in a variety of tissues including the skin, liver, lung, mammary gland and lymphoid tissue (Mirvish, 1968). A long latent period of about 1 year was generally required for tumor development. An exception was in the lung, where tumors were formed more rapidly and were manifested in about 2 to 6 months (Mirvish, 1968; Shimkin and Stoner, 1975). A similar spectrum of tumors is induced by both EC and VC. However, comparative studies revealed that VC is a more carcinogenic than EC; lung tumors induced by VC are 20- to 50-fold greater in number than are induced by EC, depending on the route of exposure (Dahl et al., 1978, 1980). Moreover, VC but not EC is mutagenic to *Salmonella typhimurium* strains TA 1535 and TA100 (Dahl et al., 1978, 1980; Leithauser et al., 1990). However, more recent studies have identified the mutagenicity of EC, using the transgenic Muta®Mouse and *lacZ* as the reporter gene (Williams et al., 1998). Nevertheless, these findings indicated that VC has greater carcinogenic potential than EC, and further that the lung is an important and possibly a primary target tissue.

Previous studies suggested that the carcinogenicity of EC is associated with its metabolism to VC and subsequently to VC epoxide (VCO), a metabolite that has been proposed to be the ultimate carcinogenic species (Dahl et al., 1978, 1980; Ribovich et al., 1982). Other studies using human liver microsomes identified oxidation of both EC and VC and implicated CYP2E1 in their metabolism (Guengerich and Kim, 1991; Guengerich et al., 1991). The results of more recent studies in murine and human lung also supported oxidation of EC and VC by the CYP2E1 enzyme (Lee and Forkert, 1997, 1999; Forkert et al., 2001). Metabolism of both EC and VC generated 1,N^6-ethenoadenosine and 3,N^4-ethenocytidine adducts in hepatic RNA and 7-(2-oxoethyl)guanine adducts in hepatic DNA of rats and mice (Ribovich, 1982; Miller and Miller, 1983; Scherer et al., 1986). In subsequent studies, VCO was synthesized and found to react with calf thymus DNA to form two major guanine adducts, N^2,3-ethenodeoxyguanosine and 7,-(2′-oxoethyl)deoxyguanosine, and one minor adenine adduct, 1,N^6-ethenodeoxyadenosine (εdAS) (Park et al., 1993). More recent studies have identified the formation of εdAS and 3,N^4-ethenodeoxycytidine in liver and lung DNA of several strains of mice treated with EC or its metabolites (Fernando et al., 1996). These data supported the proposal that VCO is a reactive species responsible for mediating DNA alkylation, leading to the formation of DNA adducts.

In this investigation, we have extended the findings of previous studies and adopted an in vitro approach for experiments designed to further elucidate the metabolism of VC and the mechanisms that mediated DNA alkylation. We have undertaken studies to test the hypothesis that oxidation of VC by CYP2E1 leads to the formation of an epoxide that alkylates DNA, resulting in the formation of εdAS in murine lung. Using an approach based on high performance liquid chromatography-mass spectrometry/mass spectrometry (LC/MS/MS), we have performed studies to determine if chemical oxidation of VC in reactions supplemented with

2′-deoxyadenosine (dAS) leads to εdAS formation. The proposed scheme for this metabolic pathway is illustrated in Fig. 1. We have subsequently carried out studies to investigate εdAS formation in incubations of murine lung microsomes with VC. The involvement of CYP2E1 in VC metabolism was also investigated using incubations of recombinant rat CYP2E1 (rCYP2E1) and lung microsomes from mice treated with the CYP2E1 inhibitor, diallyl sulfone ($DASO_2$). Our results demonstrated that VC oxidation has a critical role in εdAS formation. The εdAS adduct was also generated from VC in incubations of lung microsomes and rCYP2E1. These results demonstrated that VC oxidation, mediated mainly by CYP2E1, and subsequent DNA alkylation leads to production of εdAS in murine lung.

Materials and Methods

Chemicals and reagents. Chemicals were purchased from suppliers as follows: 2′-deoxyadenosine, 1,N^6-ethenodeoxyadenosine, NADPH, K_2HPO_4, and BSA (Sigma-Aldrich Canada Ltd., Oakville, ON, Canada); KCl, EDTA and acetonitrile (Fisher Scientific, Ottawa, ON, Canada). Synthesis of $DASO_2$ was carried out by Colour Your Enzyme (Bath, ON, Canada). Recombinant rat CYP2E1 expressed in human β-lymphoblastoid microsomes was obtained from BD Biosciences Discovery Labware (Bedford, MA). All solvents used for sample preparation and HPLC and LC-MS analyses were of HPLC grade and were purchased from Caledon Laboratories (Georgetown, ON, Canada). Details and results of the synthesis of VC and 2′-deoxy-2-deuteroethenoadenosine (DDAS) are described in the Supplemental File.

Chemical oxidation of VC and synthesis of εdAS. Oxidation of VC was performed according to the following method: VC (0.5 mM) was added to *m*-chloroperoxybenzoic acid (*m*CPBA) (0.51 mM) dissolved in CH_2Cl_2 (3.0 ml). The reaction mixture was stirred for about 25 min. During this time a saturated solution of dAS (0.2 mM) was prepared in water (3.0 ml), added to the reaction mixture, and stirred vigorously for 12 h at room temperature. The aqueous layer was then separated and the organic layer was extracted with water (3 x 3.0 ml). The combined aqueous layers were washed with ether (4 x 10 ml) to remove unreacted *m*CPBA and the side product *m*-chlorobenzoic acid. The aqueous layer was lyophilized in vacuo and resuspended in water containing 5% acetonitrile. Controls comprised of samples in which *m*CPBA or VC and *m*CPBA were omitted, were processed in parallel with the experimental samples and were subjected to identical protocols. All the samples were then subjected to HPLC analysis for purification of the εdAS adduct and subsequent analyses by LC-MS, LC-MS/MS and ^{1}H-NMR.

Animal treatment. Female CD-1 mice, weighing 25-28 g, were purchased from Charles River Canada (St. Constant, QC, Canada). The mice were maintained on a 12-h light/dark cycle and were allowed free access to water and food (Mouse Diet 5015; PMI Nutrition International Inc., Brentwood, MO). The mice were acclimatized to laboratory conditions for one week before being used for experiments. For inhibition studies, mice (n = 40) were treated with 100 mg/kg $DASO_2$ (p.o.) in water, while control mice (n=40) were treated with only water. After 2 h, the mice were sacrificed, lung tissues excised, frozen in liquid nitrogen and stored at -80^{o}C.

Preparation of microsomes. Lungs from 40 mice were pooled for each microsomal sample. This pooling is essential for obtaining sufficient tissue for preparation of the lung microsomes. Microsomes were prepared by differential centrifugation as described previously (Forkert et al., 2006). Lung tissue was minced and homogenized in 4 volumes of cold phosphate-buffered KCl (139 mM KCl, 100 mM K_2HPO_4, 1.5 mM EDTA, pH 7.4). The homogenate was subjected to centrifugation at 12,000g for 20 min at 2^{o}C. The supernatant was then centrifuged at 105,000g for 60 min. The final pellet was homogenized using 400 µl of buffer, and aliquots were frozen in liquid nitrogen and stored at -80^{o}C. Microsomal protein concentrations were determined by using the Bradford assay, using bovine serum albumin as the standard (Bradford, 1976).

Formation of εdAS in lung microsomal incubations. In the lung microsomal incubations, reaction mixtures in a total volume of 250 µl contained microsomal protein in 0.1 M phosphate buffer, pH 7.4, 1.0 mM NADPH and 12.5 mM dAS. The incubations were carried out at 37^{o}C. Following the incubation, the samples were placed on ice and 250 µl of cold acetonitrile was added. The proteins were precipitated and removed by centrifugation at 15,000g for 3 min. Experiments for determination of the protein concentration-curve were carried out with VC (1.0 mM), an incubation time of 20 min, and 0-5 mg of microsomal protein per ml. The time-course

experiments were performed with VC (1.0 mM) and 2.0 mg per ml of microsomal protein, using incubation times of 0-125 min. The concentration studies were carried out with 0-3.0 mM of VC, 2 mg per ml of microsomal protein and an incubation time of 40 min.

Formation of εdAS by rCYP2E1. Rates of formation of εdAS by CYP2E1 was determined in incubations containing recombinant rat CYP2E1 (rCYP2E1) co-expressed with NADPH-cytochrome P450 reductase. Reaction mixtures in a final volume of 250 μl of 0.1 M phospate-buffered saline, pH 7.4, contained 10 pmol rCYP2E1, 1.0 mM VC in water, and were preincubated for 3 min at 37^{o}C. The reaction was initiated by addition of 1.0 mM NADPH and the incubations were carried out for an additional 20 min. Reactions were terminated by immersion into liquid nitrogen. To determine εdAS formation as a function of rCYP2E1 enzyme levels, incubations of VC (1.0 mM) were performed with amounts of enzyme ranging from 0.25 to 60 pmol and an incubation time of 20 min. Time-course studies were carried out in the incubations of VC (1.0 mM) with rCYP2E1 (10 pmol), using incubation times of 0 to 80 min. Concentration-response studies were performed using 10 pmol of rCYP2E1, an incubation time of 20 min and VC concentrations ranging from 0 to 4.0 mM.

Formation of εdAS by lung microsomes from $DASO_2$-treated mice. Incubations with VC were performed with lung microsomes from mice that were treated 2 h previously with $DASO_2$ (100 mg/kg, p.o.) in water. Incubations with lung microsomes from mice treated with equivalent volumes of the vehicle served as controls. Reaction mixtures in a final volume of 250 μl contained microsomal protein (2.0 mg/ml) in 0.1 M phosphate buffer, pH 7.4, 1.0 mM NADPH, 12.5 mM dAS and a range of VC concentrations (0 - 3.0 mM). The incubations were carried out at 37^{o}C for 40 min.

DMD Fast Forward. Published on February 12, 2007 as DOI: 10.1124/dmd.106.013805
This article has not been copyedited and formatted. The final version may differ from this version.

HPLC purification of εdAS. Samples generated from the chemical synthesis of VCO and the rCYP2E1 incubations were redissolved in 95:5% water:acetonitrile and subjected to HPLC purification against the standards, dAS and εdAS. HPLC analysis was conducted on an Alliance 2695 separations module and 996 photodiode array detector (Waters) using a water/acetonitrile-based gradient system on a C_{18} Ultrasphere ODS column (5 μm, 4.6 mm × 25 cm; Beckman). The gradient was started at 95:5% water:acetonitrile and brought to 86:14% over 16 min at a flow rate of 0.4 ml/min. The mobile phase was returned to its initial conditions of 95:5% water:acetonitrile over 3 min at a flow rate of 0.4 ml/min and subsequently over 6 min at a flow rate of 1 ml/min. The duration of each run was 25 min. A 5.0-min time delay between samples was included to ensure proper re-equilibration of the HPLC column. Under these conditions, the authentic εdAS and the εdAS adduct eluted at 18.93 min, whereas dAS eluted at 16.87 min. Fractions that possessed identical spectral and/or chromatographic properties as the authentic εdAS were collected and samples of each type were pooled separately and evaporated to dryness.

Identification of DNA adducts. The pooled fractions from the chemical synthesis, lung microsomal incubations and the rCYP2E1 incubations were redissolved in 95:5% water:methanol and subjected to LC-MS analysis using a similar HPLC system as described above, connected in-line with a Quattro Ultima mass spectrometer (Micromass, UK) in positive ion mode (ES^+). Separation was facilitated by a gradient solvent system starting at 95:4:1% water:methanol:1% glacial acetic acid and terminating at 59:40:1 over 25 min on a Zorbax SB-C_{18} column (3.5 μm, 2.1 × 150 mm; Agilent), using a flow rate of 0.12 ml/min. Initially, the instrument was set to establish the molecular weight of the fractions in scanning or MS1 mode (set to scan from 50-600 *m/z*), against the authentic dAS, εdAS and DDAS (synthesis described above). MS2 analysis was subsequently used to establish the fragmentation pattern of the

selected MS1 parent, using collision-induced dissociation with argon gas at a pressure of 30 mbar and a collision energy of 20 eV, where specific molecular fragments were detected over a range of 50-450 *m/z*. The identification of the DNA adduct in our experimental preparations was based upon a comparison of UV spectral properties, chromatographic retention time, and characteristic ions from MS1 and MS2, with the authentic εdAS.

Quantitative analysis of DNA adducts. Samples generated from incubations of lung microsomes or rCYP2E1 were divided into two aliquots. DDAS (100 ng) was dispensed into one aliquot of each sample, as an internal standard. The aliquots were analyzed by LC-MS/MS in multiple reaction monitoring (MRM) mode, where the abundance of the characteristic MS2 ions from selected parent MS1 ions were simultaneously measured for dAS (substrate, 252→136 *m/z*), εdAS adduct (276→160 *m/z*) and DDAS (internal standard, 277→161 *m/z*). The recovery of the MRM signal from the added DDAS in one aliquot, was used to determine the amount of εdAS present in the other aliquot based upon the appropriate MRM signal, where $n = 4$ for each sample. In determining the amount of internal standard signal recovered, the confounding 277→161 *m/z* signal arising from the natural isotopic variants of εdAS, albeit negligible, was subtracted, based upon the abundance of 277→161 *m/z* arising from the aliquots to which no internal standard was added.

Statistical analysis. Data were expressed as mean ± S.E.M. Data analysis including curve fitting analysis of VC concentration data was performed using GraphPad Prism version 4 (GraphPad Software Inc., San Diego, CA).

Results

Identification of εdAS by LC-MS/MS. In this study, we have developed a LC-MS/MS protocol to establish the identity of the DNA adduct formed in incubations of VC with lung microsomes and rCYP2E1 as well as under conditions of VC oxidation using *m*CPBA. The MS1 mass spectral analysis of dAS revealed the molecular ion *m/z* 252 $[M+H]^+$ (Fig. 2A). Similar analysis for the authentic εdAS, which was used as the standard, was identified by the molecular ion *m/z* 276 (Fig. 2B). The synthesized DDAS applied as the internal standard, was characterized by the production of the molecular ion *m/z* 277, which accounts for the introduction of a single deuterium atom at C2 (Fig. 2C). Subsequent MS2 analysis of the fragments for dAS, the authentic εdAS and DDAS yielded the specific fragment ions *m/z* 136 (Fig. 2D), *m/z* 160 (Fig. 2E) and *m/z* 161 (Fig. 2F), respectively. It should be noted that no ions corresponding to the sugar backbone cleavage fragment were detected in MS2 mode. Based upon the MS1 and MS2 data, the following MRM transitions were established in order to selectively identify and quantitate the nucleotides under investigation: dAS: 252→136, εdAS: 276→160, DDAS: 277→161. Mass spectral analysis of the DNA adduct generated in incubations of VC with lung microsomes in the presence of dAS, or similar incubations with rCYP2E1, produced the major molecular ion *m/z* 276$[M+H]^+$ (Fig. 3, A and B), identical to that of the authentic εdAS (Fig. 2B). MS2 analysis revealed a specific fragment *m/z* 160 for the εdAS adduct generated in incubations of VC with lung microsomes (Fig. 3D) or rCYP2E1 (Fig. 3E). The difference in the *m/z* ratio between dAS and εdAS produced in the incubations of VC with lung microsomes and rCYP2E1 (24 mass units) corresponded with the change in molecular weight predicted for the formation of the 1,N^6-etheno adduct of dAS. The same difference in *m/z*

ratio was observed among the MS2 fragments, which resulted from cleavage of the anomeric C-N bond.

Representative MRM chromatograms of the standards and experimental preparations are shown in Fig. 4. Typically, DDAS (18.60 min) eluted 0.2-0.3 minutes earlier than the authentic εdAS (18.93 min). The slight discrepancy between the retention time of the authentic εdAS and the adduct detected by the same MRM transition in the microsomal and rCYP2E1 incubations (0.32-0.33 min) is due to the presence of excess dAS in the sample, even after an initial HPLC purification step prior to LC-MS-MS. Some contaminating dAS (*m/z* 252) in the pre-purified adduct sample derived from incubations with rCYP2E1 was also evident (Fig. 4B). Taken together, the chromatographic retention times, and characteristic MS1 and MS2 ions confirmed that εdAS is produced in incubations of VC and dAS with both lung microsomes and rCYP2E1.

Chemical oxidation of VC and synthesis of εdAS. The DNA adduct produced from dAS in the presence of VC oxidized with *m*CPBA produced identical MS1 and MS2 spectra (Fig 3, C and F), similar to those for the authentic εdAS (Fig. 2, B and E). The spectra were also similar to those obtained in the incubations of VC with lung microsomes (Fig. 3, A and D) and with rCYP2E1 (Fig. 3, B and E). The chromatographic retention time for εdAS formed under the oxidative conditions of VC was 18.60 min, and was similar to those identified for the adduct produced in the lung microsomal and rCYP2E1 incubations, which were 18.61 min and 18.76 min, respectively (Fig. 4B). No εdAS adduct was produced in the controls in which reactions were carried out in the absence of *m*CPBA or of VC and *m*CPBA.

The identity of the εdAS adduct formed via chemical oxidation of VC in the presence of dAS was confirmed by the spectroscopic data: ^{1}H-NMR (600 MHz, D_2O): 9.08 (1H, s, H_2), 8.37 (1H, s, H_8), 7.94 (1H, s, H_{10} or H_{11}), 7.53 (1H, s, H_{10} or H_{11}), 6.54 (1H, t, J=6.6Hz, $H_{1'}$), 4.10 (1H, m,

DMD Fast Forward. Published on February 12, 2007 as DOI: 10.1124/dmd.106.013805
This article has not been copyedited and formatted. The final version may differ from this version.

$H_{4'}$), 3.76 (1H, dd, J=12.6, 3.4Hz, $H_{5a'}$), 3.70 (1H, dd, J=12.6, 4.7Hz, $H_{5b'}$), 2.87 (1H, pentet, J=13.8, 6.8Hz, $H_{2a'}$), 2.55 (1H, m, $H_{2b'}$). These spectroscopic data are in agreement with those obtained for the authentic εdAS: ^{1}H-NMR (400 MHz, D_2O): 9.10 (1H, s, H_2), 8.42 (1H, s, H_8), 7.97 (1H, s, H_{10} or H_{11}), 7.58 (1H, s, H_{10} or H_{11}), 6.59 (1H, t, J=6.6Hz, $H_{1'}$), 4.70 (1H, m, $H_{3'}$), 4.19 (1H, m, $H_{4'}$), 3.85 (1H, dd, J=12.5, 3.5Hz, $H_{5a'}$) 3.79 (1H, dd, J=12.5, 4.9Hz, $H_{5b'}$), 2.94 (1H, pentet, J=14, 6.8Hz, $H_{2a'}$), 2.63 (1H, ddd, J=14, 6.3, 3.9Hz, $H_{2b'}$).

Formation of εdAS in lung microsomal incubations. Incubations of lung microsomes with VC and NADPH showed that εdAS formation was dependent on protein concentrations ranging from 0 to 5.0 mg per ml (Fig. 5A). Peak adduct formation was found in incubations containing 3.0 mg of microsomal protein. In time-dependent studies, εdAS production from VC was incremental from 0 to 60 min. Prolongation of the incubation time to 125 min resulted in no further increase in εdAS production but rather resulted in a decline (Fig. 5B). Based on the data obtained from the protein concentration and time-course studies, microsomal incubations with a range of VC concentrations were carried out under conditions of linearity, and were performed with 2.0 mg per ml of microsomal protein and an incubation time of 40 min. The rates of εdAS formation were highly correlated (R^2 = 0.9940) with VC concentrations (0.25 – 3.0 mM) used in the microsomal incubations (Fig. 5C). The peak rate (210.8 ± 4.8 pmol/min/nmol P450) of εdAS production in the incubations was achieved at a VC concentration of 3.0 mM.

Formation of εdAS by rCYP2E1. Formation of εdAS was detected in incubations of rCYP2E1 with VC. Production of εdAS was dependent on rCYP2E1 concentrations of 2.5 to 40 pmol used in the incubations (Fig. 6A). Although maximal εdAS formation was achieved in incubations containing 40 pmol of rCYP2E1, saturation was found at about 20 pmol of enzyme. In time-course experiments, εdAS formation was dependent on the duration of the incubations,

DMD Fast Forward. Published on February 12, 2007 as DOI: 10.1124/dmd.106.013805
This article has not been copyedited and formatted. The final version may differ from this version.

and was incremental from 0 to 30 min (Fig. 6B). Adduct formation reached saturation at incubation times of 30 to 60 min, and declined at 80 min. On the basis of these data, incubations of rCYP2E1 with a range of concentrations of VC (0.25 - 4.0 mM) were carried out under conditions of linearity, and were performed for 20 min, using 10 pmol of rCYP2E1 enzyme. The rates of εdAS production increased between VC concentrations of 0.25 to 2.5 mM, achieved saturation at a concentration of 2.5 mM (207.7 ± 21.7 pmol/min/10 pmol rCYP2E1) and remained at a plateau from 2.5 to 4.0 mM. The results demonstrated a high correlation (R^2 = 0.9108) between the rates of εdAS formation and the concentrations of VC used in the incubations (Fig. 6C).

Formation of εdAS by lung microsomes from $DASO_2$-treated mice. Incubations with VC (0 – 3.0 mM) were also carried out with lung microsomes from control mice and mice treated with $DASO_2$ (100 mg/kg, p.o.). In incubations of control lung microsomes with VC, the levels of εdAS formation were concentration-dependent and were maximal in reactions containing the highest VC concentration of 3.0 mM (Fig. 7). Regression analysis revealed a high correlation (R^2 = 0.9510) between the VC concentrations used in the incubations and magnitudes of εdAS formation. In incubations of lung microsomes from $DASO_2$-treated mice, the levels of εdAS formation were also concentration-dependent but were lower than in incubations using microsomes from the untreated controls. Regression analysis also showed a high correlation (R^2 = 0.9883) between VC concentrations and production of εdAS. Comparative analysis of εdAS levels in the lung microsomal incubations revealed significant decreases in all the incubations containing microsomes from $DASO_2$-treated mice, relative to the controls. The extent of inhibition by $DASO_2$ was similar regardless of the VC concentrations used in the microsomal

incubations; a decrease of about 70% of the control levels was detected for all VC concentrations.

DMD Fast Forward. Published on February 12, 2007 as DOI: 10.1124/dmd.106.013805
This article has not been copyedited and formatted. The final version may differ from this version.

Discussion

This study has produced definitive physico-chemical data that have validated our working hypothesis that oxidation of VC leads to the formation of VCO that can alkylate DNA to form εdAS (Fig. 1). We have adopted an approach using LC-MS and LC-MS/MS to investigate formation of εdAS from VC. The identification of εdAS was confirmed and based on the MS1 (*m/z* 276) and MS2 (*m/z* 160) ions (Figs. 2, B and E, and Fig. 3), as well as the chromatographic retention times of the samples (Fig. 4). A critical component of this study was the synthesis of the internal standard DDAS ((Fig. 2, C and F), which was integral to quantitation of the formation of εdAS under various experimental conditions. In conjunction with NMR analysis, the results have provided validation for the application of the LC-MS and LC-MS/MS approach for qualitative and quantitative characterization of the εdAS adduct.

An important objective of this study was to confirm that oxidation of VC leads to the production of a metabolite, presumably the reactive VCO, which reacts with DNA to form εdAS (Fig. 1). We have carried out chemical experiments in which VC was oxidized with *m*CPBA and then reacted with dAS. The DNA adduct produced from this reaction demonstrated similar mass spectral (Fig. 3, C and F) and chromatographic properties (Fig. 4B) as the authentic εdAS (Fig. 2, B and E), thus confirming that εdAS was formed. In the biological experiments, chromatographic and mass spectral analyses of samples from the lung microsomal incubations supplemented with dAS confirmed that the εdAS adduct was generated from VC in a manner that was dependent on protein concentrations (Fig. 5A) and incubation time (Fig. 5B). The production of εdAS was highly correlated (R^2 = 0.9940) with VC concentrations (Fig. 5C). These results have established the ability of lung microsomes to catalyze P450-dependent formation of εdAS in our experiments. Furthermore, our results have shown that εdAS

production in incubations of VC with rCYP2E1 was dependent on enzyme concentrations (Fig. 6A) and incubation time (Fig. 6B), and was highly correlated (R^2 = 0.9108) with VC concentrations (Fig. 6C). Taken together, these findings have provided evidence to support a role for CYP2E1 in VC oxidation and the subsequent production of εdAS (Fig. 1).

Previous studies have identified the garlic constituent $DASO_2$ as an inhibitor of the CYP2E1 enzyme in the lungs of mice (Forkert et al., 1996). Treatment of mice with $DASO_2$ (100 mg/kg, p.o.) elicited a 75% inhibition of lung *p*-nitrophenol (PNP) hydroxylation, a catalytic activity associated with CYP2E1. The loss of PNP hydroxylase activity coincided with a decrease in immunodetectable lung microsomal CYP2E1 protein. Hydroxylation of chlorxozazone, a prototypic substrate for the CYP2E1 enzyme, was decreased by 60% in lung microsomes from mice treated with $DASO_2$ (100 mg/kg, p.o.) (Simmonds et al., 2004a). The mechanism of CYP2E1 inactivation has been ascribed to formation of an epoxide (1,2-epoxypropyl-3,3′-sulfonyl-1′-propene) from oxidation of $DASO_2$, leading, in part, to production of the heme adduct *N*-alkylprotoporphyrin IX in incubations of lung microsomes or recombinant rat CYP2E1 (Forkert et al., 2000; Black et al., 2006). These findings implicated CYP2E1 in the metabolism of $DASO_2$, resulting in CYP2E1 inactivation and inhibition of the metabolism of CYP2E1 substrates. Here, we have carried out inhibitory studies using $DASO_2$ to verify that CYP2E1 catalyzes the formation of εdAS under biological conditions. The results showed significant inhibition of εdAS formation in incubations of VC (0.25-3.0 mM) with lung microsomes from $DASO_2$-treated (100 mg/kg, p.o.) mice (Fig. 7). Irrespective of the amounts of VC used in the incubations, the extent of inhibition was about 70% of the corresponding control levels, suggesting that this was the maximum extent inhibitable by $DASO_2$. Taken together, these data

suggested that CYP2E1 is responsible, in large measure, for the production of εdAS in the lung microsomal incubations.

Although our CYP2E1 inhibition studies with $DASO_2$ supported the role of this P450 in catalyzing the formation of VCO and subsequently εdAS, the specificity of the inhibitory effect of $DASO_2$ on P450 enzymes must also be addressed. We have previously determined the effects of $DASO_2$ on the rates of PNP hydroxylation by rCYP2E1 and recombinant goat CYP2F3 (rCYP2F3). The results showed that incubation of rCYP2E1 and rCYP2F3 with $DASO_2$ decreased hydroxylase activities by 90 and 70%, respectively (Simmonds et al., 2004a). Moreover, incubation of $DASO_2$ with rCYP2E1 and rCYP2F3 decreased hydroxylation of chlorzoxazone by 90 and 77%, respectively. These findings demonstrated that $DASO_2$ inhibited both CYP2E1 and CYP2F3, and additionally suggested the possibility that the CYP2F enzyme, in addition to CYP2E1, may be involved in VC metabolism. In light of these data and our current observation that 30% of the activity remained after maximal inhibition with $DASO_2$ (Fig. 7), we carried out preliminary experiments to determine if recombinant mouse CYP2F2 or recombinant rat CYP2F4 could also be involved in VC metabolism, leading to εdAS formation. The CYP2F enzyme is expressed selectively in the lung, with relatively little expression in the liver (Hakkola et al., 1994; Shultz et al., 1999). We have incubated VC (1.0 mM) and dAS (12.5 mM) with amounts of recombinant mouse CYP2F2 and recombinant rat CYP2F4 ranging from 0.25 to 40 pmol, using procedures described previously (Simmonds et al., 2004b). Our chromatographic and mass spectral analysis failed to detect formation of the εdAS adduct by either the rCYP2F2 or the rCYP2F4 enzymes. Taken together, these findings suggested that CYP2E1 plays a major role in the production of εdAS in the lung microsomal incubations.

These results do not, however, preclude the participation of other P450 isoforms, as yet unidentified, in VC metabolism.

The human relevance of the studies with VC and EC has a historical perspective. EC was used as a co-solvent for analgesic and sedative drugs in Japan between 1950 and 1975, and it was estimated that the total dose of EC administered to a 60-kg patient was about 0.6 to 3.0 g (Nomura, 1975). This period represented 25 years during which millions of humans were administered "the largest doses of a pure carcinogen that is on record" (Miller, 1991). Today, human exposures occur inadvertently via the consumption of fermented foods and alcoholic beverages (Battaglia et al., 1990; Ough 1976). In this study, the results from incubations of lung microsomes with VC revealed that the rate of εdAS production was not fully saturated at a concentration of 3.0 mM (Fig. 5C). In the case of the incubations of rCYP2E1 with VC, saturation was achieved at a concentration of 2.5 mM. These findings suggested that formation of εdAS occurs at a slow rate and at relatively high VC concentrations, suggesting that VC may not pose a carcinogenic risk in humans as exposures are predictably at extremely low levels, especially when VC exposure is via generation from EC. However, the potential adverse effects of VC exposure in human lung remain to be investigated and characterized. Nonetheless, in reference to EC, Miller and Miller (1983) have reiterated that "it is possible that even low life-time intakes of so-called "weak" carcinogens could induce cancers in some humans with especially predisposing genetic backgrounds and dietary habits". Ethyl carbamate has exhibited moderate-to-weak carcinogenic activity in experimental animals.

The results of this investigation have demonstrated the ability of lung microsomes to catalyze the oxidation of VC via CYP2E1, resulting in the production of εdAS. This finding is consistent with data from previous in vivo studies that identified εdAS and 3,N^4-ethenodeoxycytidine in

liver and lung DNA of mice treated with EC or VC (Fernando et al., 1996; Titis and Forkert, 2001). Both carbamate compounds also formed 7-(2'-oxoethyl)deoxyguanosine and εdAS in liver DNA of rodents (Ribovich et al., 1982; Scherer et al., 1986; Miller and Miller, 1983). Although 7-(2'-oxoethyl)deoxyguanosine comprises 98% of total adducts in hepatic DNA, the minor lesion affecting εdAS has been regarded as significant because of its ability to miscode in transcription of DNA (Barbin and Bartsch, 1986; Basu et al., 1993). The propensity for the miscoding in DNA transcription is associated with base changes such as A→G and A→T in mammalian cells (Pandya and Moriya, 1996). Our finding of εdAS formation in the lung has provided a vital link to data from our recent studies showing high frequencies of A:T→G:C and A:T→T:A mutations in the lungs of VC-treated mice (Hernandez and Forkert, 2007). Although similar types of mutations were generated by VC and EC, the incidences of mutant frequencies as induced by VC required an EC dose that was 17-fold higher, thus confirming the greater carcinogenic potential of VC vs. EC. In this regard, VC has been found to elicit not only a high frequency of mutations, but is also active in inducing micronuclei and sister chromatid exchange (Dahl et al., 1978, 1980; Allen et al., 1982; Hernandez and Forkert, 2007; Wild, 1991). In summary, our results have shown formation of εdAS as a result of VC oxidation by CYP2E1, and supported the contention that such a mechanism is the underlying molecular event for the DNA damage sustained by animals treated with VC that ultimately results in lung tumor development.

Acknowledgments

We wish to thank Dr. Francoise Sauriol for the 600 MHz ^{1}H-NMR spectrum. We also wish to thank Drs. Alan Buckpitt, Michael Shultz and Michael Baldwin for their contribution of recombinant CYP2F2 and recombinant CYP2F4 for our preliminary studies.

References

Allen JW, Langenbach R, Nesow S, Sasseville K, Leavitt S, Campbell J, Brock K, and Sharief Y (1982) Comparative genotoxicity studies of ethyl carbamate and related chemicals: further support for vinyl carbamate as a proximate carcinogenic metabolite. *Carcinogenesis* **3:**1437-1441.

Barbin A and Bartsch H (1986) Mutagenic and promutagenic properties of DNA adducts formed by vinyl chloride metabolites, in *The Role of Cyclic Nucleic Acid Adducts in Carcinogenesis and Mutagenesis* (Singer B and Bartsch H eds) pp 345-358, IARC Scientific Publications No. 70, International Agency for Research on Cancer, Lyon.

Basu AK, Wood ML, Neidernhofer LJ, Ramos LA, and Essigmann JM (1993) Mutagenic and genotoxic effects of three vinyl chloride-induced DNA lesions: 1,N^6-ethenoadenine, 3,N^4-ethenocytosine and 4-amino-5-(imidazol-2-yl)imidazole. *Biochemistry* **32**:12793-12801.

Battaglia R, Conacher BS, and Page BD (1990) Ethyl carbamate (urethane) in alcoholic beverages and foods: a review. *Food Add Contaminants* **7:**477-496.

Black GP, Collins KS, Blacquiere DP, and Forkert PG (2006) Formation of *N*-alkylprotoporphyrin IX from metabolism of diallyl sulfone in lung and liver. *Drug Metab Dispos* **34:**895-900.

Bradford MM (1976) A rapid and sensitive method for the quantitation of microgram quantities of protein utilizing the principle of protein-dye binding. *Anal Biochem* **72:**248-254.

Dahl GA, Miller JA, and Miller EC (1978) Vinyl carbamate as a promutagen and a more carcinogenic analog of ethyl carbamate. *Cancer Res* **38:**3793-3804.

Dahl GA, Miller EC, and Miller JA (1980) Comparative carcinogenicities and mutagenicities of vinyl carbamate, ethyl carbamate, and ethyl N-hydroxycarbamate. *Cancer Res* **40:**1194-1203.

Fernando RC, Nair J, Barbin A, Miller JA, and Bartsch H (1996) Detection of 1,N^6-ethenodeoxyadenosine and 3,N^4-ethenocytidine by immunoaffinity/^{32}P-postlabelling in liver and lung DNA of mice treated with ethyl carbamate (urethane) or its metabolites. *Carcinogenesis* **17:**1711-1718.

Forkert PG, Lee RP, Dowsley TF, Hong J-Y, and Ulreich JB (1996) Protection from 1,1-dichloroethylene-induced Clara cell injury by diallyl sulfone, a derivative of garlic. *J Pharmacol Exp Ther* **277:**1665-1671.

Forkert PG, Lee RP, and Reid K (2001) Involvement of CYP2E1 and carboxylesterase enzymes in vinyl carbamate metabolism in human lung microsomes. *Drug Metab Dispos* **29:**258-263.

Forkert PG, Millen B, Lash LH, Putt DA, and Ghanayem BI (2006) Pulmonary bronchiolar cytotoxicity and formation of dichloroacetyl lysine protein adducts in mice treated with trichloroethylene. *J Pharmacol Exp Ther* **316:**520-529.

Forkert PG, Premdas PD, and Bowers RJ (2000) Epoxide formation from diallyl sulfone is associated with CYP2E1 inactivation in murine and human lungs. *Am J Respir Cell Mol Biol* **23:**687-695.

Guengerich FP, Kim D-H, and Iwasaki M (1991) Role of human cytochrome P-450 IIE1 in the oxidation of many low molecular weight cancer suscepts. *Chem Res Toxicol* **4:**168-179.

Guengerich FP and Kim DH (1991) Enzymatic oxidation of ethyl carbamate and its role as an intermediate in the formation of 1,N^6-ethenoadenosine. *Chem Res Toxicol* **4:**413-421.

Hakkola J, Pasanen R, Purkunen R, Saarikoski S, Pelkonen O, Maenpaa J, Rane A, and Raunio H (1994) Expression of xenobiotic-metabolizing cytochrome P-450 forms in human adult and fetal liver. *Biochem Pharmacol* **48:**59-64.

Hernandez LG and Forkert PG. *In vivo* mutagenicity of vinyl carbamate and ethyl carbamate in lung and small intestine of F_1 (Big Blue® x A/J) transgenic mice. *Int. J. Cancer*. DOI 10.1002/ijc.22502.

Lee RP and Forkert PG (1997) Metabolism of ethyl carbamate by pulmonary cytochrome P450 and carboxylesterase isozymes: involvement of CYP2E1 and hydrolase A. *Toxicol Appl Pharmacol* **146:**245-254.

Lee RP and Forkert PG (1999) Inactivation of cytochrome P-450 (CYP2E1) and carboxylesterase (Hydrolase A) enzymes by vinyl carbamate in murine pulmonary microsomes. *Drug Metab Dispos* **27:**233-239.

Leithauser MT, Liem A, Stewart BC, Miller EC, and Miller JA (1990) 1,N^6-Ethenoadenosine formation, mutagenicity and murine tumor induction as indicators of the generation of an electrophilic epoxide metabolite of the closely related carcinogens ethyl carbamate (urethane) and vinyl carbamate. *Carcinogenesis* **11:**463-473.

Miller JA (1991) The need for epidemiological studies of the medical exposures of Japanese patients to the carcinogen ethyl carbamate (urethane) from 1950 to 1975. *Jpn J Cancer Res* **82:**1323-1324.

Miller JA and Miller EC (1983) The metabolic activation and nucleic acid adducts of naturally occurring carcinogens: recent results with ethyl carbamate and the spice flavors safrole and estragole. *Brit J Cancer* **48:**1-15.

Mirvish SS (1968) The carcinogenic action and metabolism of urethan and *N*-hydroxyurethan. *Adv Cancer Res* **11:**1-42.

Nettleship A, Henshaw PS, and Meyer HL (1943) Introduction of pulmonary tumors in mice with ethyl carbamate (urethane). *J Natl Cancer Inst* **4:**309-319.

Nomura T (1975) Urethane (ethyl carbamate) as a co-solvent of drugs commonly used parenterally in humans. *Cancer Res* **35:**2895-2899.

Ough CS (1976) Ethyl carbamate in fermented beverages and foods. I. Naturally occurring ethyl carbamate. *Agric Food Chem* **24:**323-328.

Pandya GA and Moriya M (1996) 1,N^6-ethenodeoxyadenosine, a DNA adduct highly mutagenic in mammalian cells. *J Agric Food Chem* **24:**323-328.

Park KK, Surh YJ, Steward BC, and Miller JA (1990) Synthesis and properties of vinyl carbamate epoxide, a possible ultimate electrophilic and carcinogenic metabolite of vinyl carbamate and ethyl carbamate. *Biochem Biophys Res Commun* **169:**1094-1098.

Ribovich ML, Miller JA, Miller EC, and Timmins LG (1982) Labeled 1, N^6-ethenoadenosine and 3,N^4-ethenocytidine in hepatic RNA of mice given [ethyl-1,2-^{3}H] or [ethyl-1-^{14}C]ethyl carbamate (urethan). *Carcinogenesis* **3:**539-546.

Scherer E, Winterwerp H, and Emmelot P (1986) Modification of DNA and metabolism of ethyl carbamate *in vivo*: formation of 7-(2-oxoethyl)-guanine and its sensitive determination by reductive tritiation using ^{3}H sodium borohydride, in *The Role of Cyclic Nucleic Acid Adducts in Carcinogenesis and Mutagenesis* (Singer B and Bartsch H eds), pp 109-125, IARC Scientific Publications No. 70, International Agency for Research on Cancer, Lyon.

Schmeltz I, Chiong KG, and Hoffmann D (1978) Formation and determination of ethyl carbamate in tobacco and tobacco smoke. *J Anal Toxicol* **2:**265-268.

Shimkin MB and Stoner GD (1975) Lung tumors in mice: application to carcinogenesis bioassay. *Adv Cancer Res* **21:**1-58.

Shultz MA, Choudary PV, and Buckpitt AR (1999) Role of murine cytochrome P-450 2F2 in metabolic activation of naphthalene and metabolism of other xenobiotics. *J Pharmacol Exp Ther* **290:**281-288.

Simmonds AC, Ghanayem BI, Sharma A, Reilly CA, Millen B, Yost G, and Forkert PG (2004a) Bioactivation of 1,1-dichloroethylene by CYP2E1 and CYP2F2 in murine lung. *J Pharmacol Exp Ther* **310:**855-864.

Simmonds AC, Reilly CA, Baldwin RM, Ghanayem BI, Lanza DL, Yost GS, Collins KS and Forkert PG (2004b) Bioactivation of 1,1-dichloroethylene to its epoxide by CYP2E1 and CYP2F enzymes. *Drug Metab Dispos* **32:**1032-1039.

Titis AP and Forkert PG (2001) Strain-related differences in bioactivation of vinyl carbamate and formation of DNA adducts in lungs of A/J, CD-1, and C57BL/6 mice. *Toxicol Sci* **59:**82-91.

Wild D (1991) Micronucleus induction in bone marrow by vinyl carbamate, a hypothetical metabolite of the carcinogen urethane (ethyl carbamate). *Mutat Res* **260:**309-310.

Williams CV, Fletcher K, and Ashby J (1998) Mutagenicity of ethyl carbamate to *lacZ*⁻ transgenic mice. *Mutagenesis* **13:**133-137.

Zimmerli B and Schlatter J (1991) Ethyl carbamate: analytical methodology, occurrence, formation, biological activity and risk assessment. *Mutat Res* **259:**325-350.

Footnotes

a) This study was funded by the Canadian Cancer Society through Grant # 014061 from the National Cancer Institute of Canada (to P.G.F.). Funding for the Mass Spectrometer (LC-MS/MS) and for the Service Contract on the LC-MS/MS was provided by Grant MA-9475 and Grant MMA-69106, respectively, from the CIHR (to G.J.). M.K. was supported by an Ontario Graduate Scholarship. A.S. was supported by postdoctoral fellowships from the Cancer Research Society and Queen's University Principal's Development Fund.

b) Address correspondence to: Dr. Poh-Gek Forkert, Department of Anatomy and Cell Biology, Queen's University, Kingston, Ontario, Canada K7L 3N6.

Email: forkertp@post.queensu.ca

Figure Legends

Fig. 1. Proposed scheme of EC metabolism to VC and the formation of 1,N^6-ethenodeoxyadenosine from reaction of VC epoxide with 2′-deoxyadenosine.

Fig. 2. Standards used for identification and quantitation of the εdAS adduct. Samples were analyzed by LC-MS/MS in multiple reaction mode, where the abundance of the characteristic MS2 ions (D-F) from selected parent MS1 ions (A-C) were measured for dAS (A), the authentic εdAS used as a standard (B) and DDAS used as the internal standard (C).

Fig. 3. Mass spectral analyses of chemical and biological samples for formation of εdAS. The εdAS adduct was identified on the basis of its characteristic MS1 spectra (A-C) and MS2 fragmentation patterns (D-F) in ES+ mode. The εdAS adduct was generated in incubations of VC with lung microsomes (A and D), in incubations of VC with rCYP2E1 (B and E) or synthesized by VC oxidation, using *m*CPBA, in the presence of dAS (C and F).

Fig. 4. Retention times were derived from LC-MS/MS analysis of the standards (A): dAS (*m/z* 252→136), authentic εdAS used as the standard (*m/z* 276→160) and DDAS used as the internal standard (*m/z* 277→161). Retention times were also derived for the products generated in the experimental preparations (B): VC oxidation (VCO) in the presence of dAS (*m/z* 276→160), incubations of lung microsomes with VC (*m/z* 276→160), and incubations of rCYP2E1 with VC (*m/z* 276→160). The arrows represent the proposed sites of cleavage at the anomeric centres of dAS, εdAS or DDAS (A).

Fig. 5. Formation of εdAS in incubations of murine lung microsomes with VC. Studies of protein concentrations were carried out using 0 to 5 mg of microsomal protein, 1.0 mM of VC and an incubation time of 20 min (A). Time-dependent studies were performed using 2.0 mg of

microsomal protein, 1.0 mM of VC and incubation times of 0 to 125 min (B). Concentration-dependent studies were carried out using 2.0 mg per ml of microsomal protein, an incubation time of 40 min and VC concentrations ranging from 0 to 3.0 mM (C). All incubations contained 1.0 mM of NADPH and were carried out at 37^{o}C.

Fig. 6. Formation of εdAS in incubations of rCYP2E1 with VC. Studies of rCYP2E1 concentrations were carried out with 0 to 60 pmol of enzyme, 1.0 mM of VC and an incubation time of 20 min (A). Time-course studies were performed with 10 pmol of rCYP2E1, 1.0 mM of VC and incubation times of 0 to 80 min (B). Concentration-dependent studies were carried out with 10 pmol of rCYP2E1, VC concentrations ranging between 0 and 4.0 mM and an incubation time of 20 min (C). All incubations contained 1.0 mM of NADPH and were carried out at 37^{o}C.

Fig. 7. Formation of εdAS in incubations of VC with lung microsomes from control and $DASO_2$-treated mice. Mice were treated with $DASO_2$ (100 mg/kg, p.o.), while control mice were treated with water. All mice were sacrificed 2 h later for isolation of lung microsomes. Reaction mixtures in a final volume of 250 μl contained microsomal protein (0.5 mg) in 0.1 M phosphate buffer, pH 7.4, 1.0 mM NADPH, 12.5 mM dAs and VC (0 - 3.0 mM). The microsomal incubations were carried out for 40 min at 37^{o}C. The correlation of variation was R^2 = 0.9510 and R^2 = 0.9883 for control and $DASO_2$-treated mice, respectively.

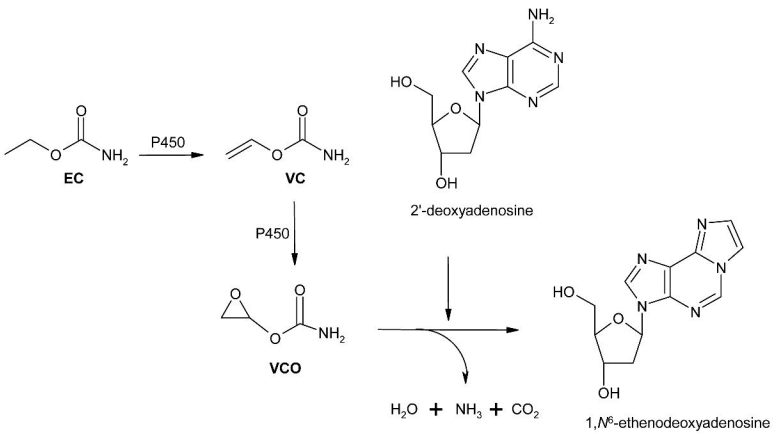
EC
P450
VC
P450
VCO
2'-deoxyadenosine
H_2O + NH_3 + CO_2
1,N^6-ethenodeoxyadenosine

Figure 1

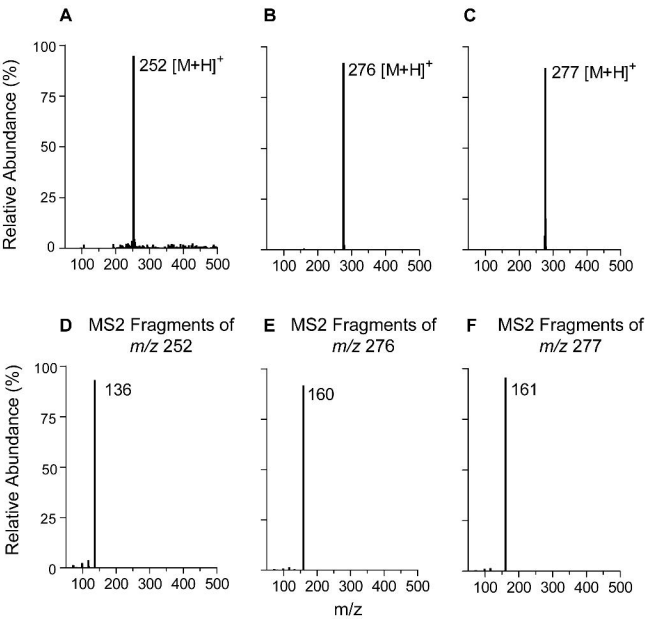
A
B
C
252 [M+H]+
276 [M+H]+
277 [M+H]+
Relative Abundance (%)
100
75
50
25
0
100 200 300 400 500
D MS2 Fragments of m/z 252
E MS2 Fragments of m/z 276
F MS2 Fragments of m/z 277
136
160
161
m/z

Figure 2

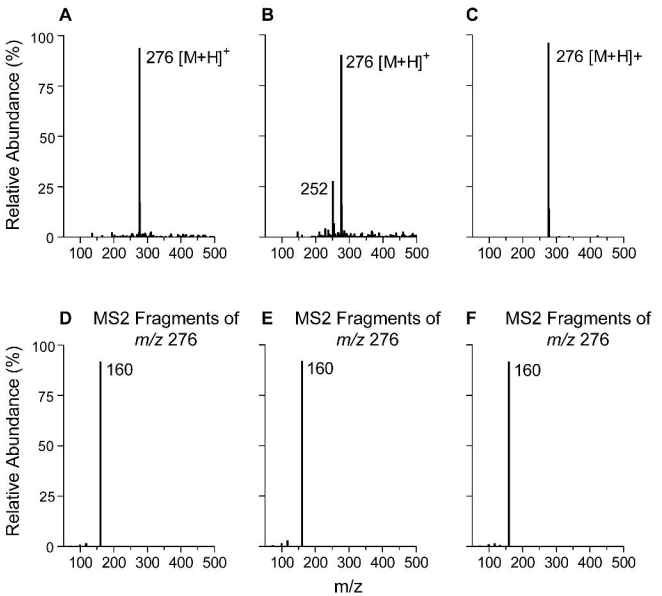
A
B
C
276 [M+H]+
276 [M+H]+
276 [M+H]+
252
Relative Abundance (%)
100
75
50
25
0
100 200 300 400 500
D MS2 Fragments of m/z 276
E MS2 Fragments of m/z 276
F MS2 Fragments of m/z 276
160
160
160
m/z

Figure 3

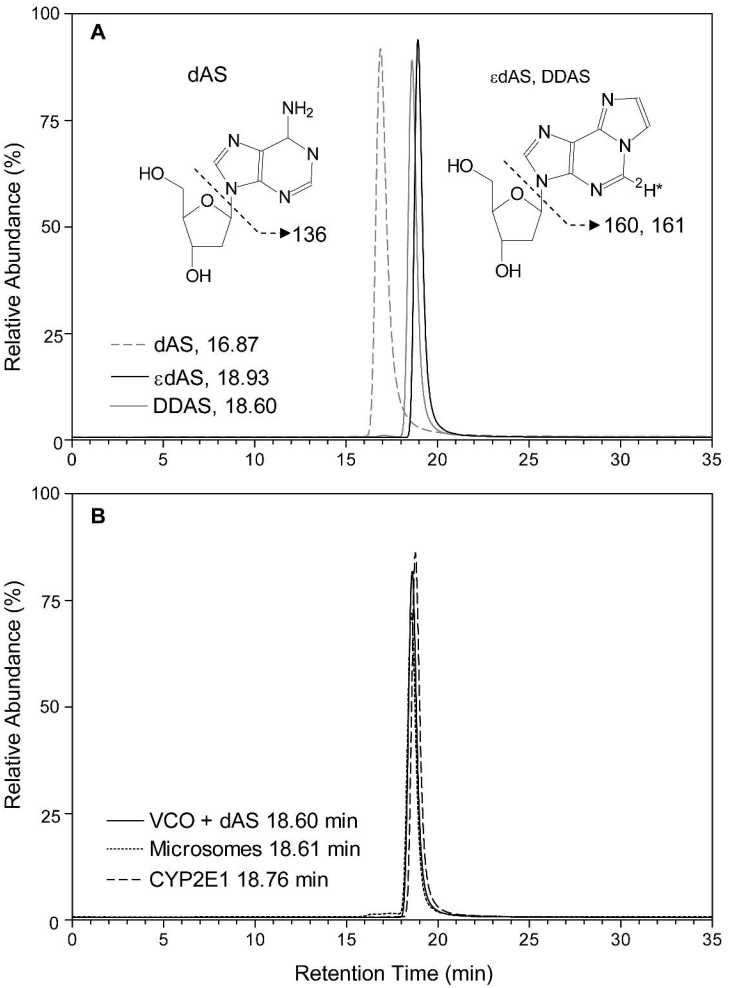
A
dAS
NH2
HO
O
OH
136
εdAS, DDAS
2H*
160, 161
dAS, 16.87
εdAS, 18.93
DDAS, 18.60
Relative Abundance (%)
B
VCO + dAS 18.60 min
Microsomes 18.61 min
CYP2E1 18.76 min
Retention Time (min)

Figure 4

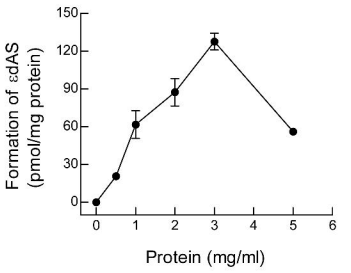
Formation of εdAS
(pmol/mg protein)
150
120
90
60
30
0
0
1
2
3
4
5
6
Protein (mg/ml)

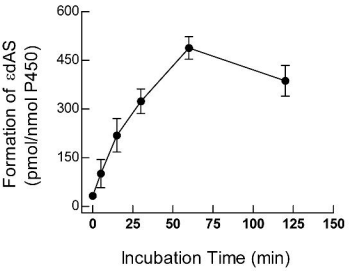
Formation of εdAS
(pmol/nmol P450)
600
450
300
150
0
0
25
50
75
100
125
150
Incubation Time (min)

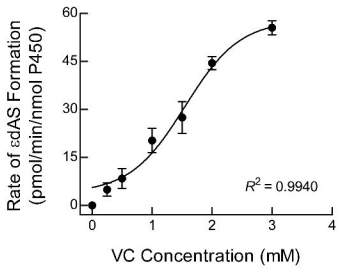
Rate of εdAS Formation
(pmol/min/nmol P450)
60
45
30
15
0
0
1
2
3
4
R^2 = 0.9940
VC Concentration (mM)

Figure 5

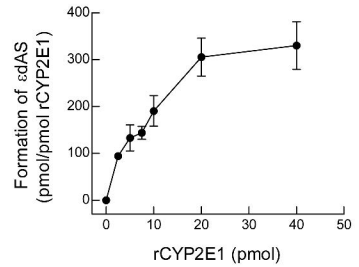
Formation of εdAS (pmol/pmol rCYP2E1)
400
300
200
100
0
0
10
20
30
40
50
rCYP2E1 (pmol)

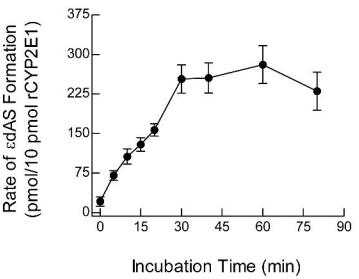
Rate of εdAS Formation (pmol/10 pmol rCYP2E1)
375
300
225
150
75
0
0
15
30
45
60
75
90
Incubation Time (min)

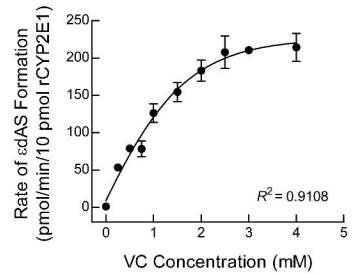
Rate of εdAS Formation (pmol/min/10 pmol rCYP2E1)
250
200
150
100
50
0
R^2 = 0.9108
0
1
2
3
4
5
VC Concentration (mM)

Figure 6

DMD Fast Forward. Published on February 12, 2007 as DOI: 10.1124/dmd.106.013805
This article has not been copyedited and formatted. The final version may differ from this version.

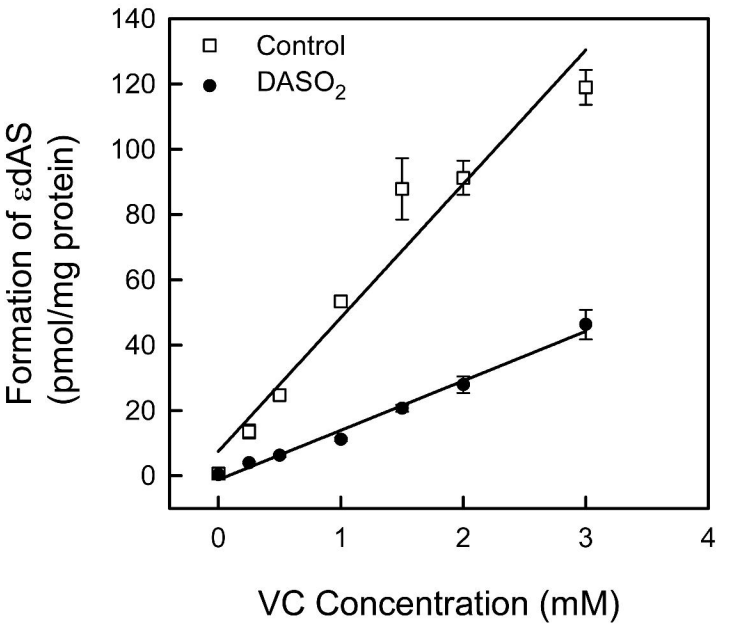

Figure 7